Journal of King Saud University – Computer and Information Sciences xxx (xxxx) xxx

Contents lists available at ScienceDirect

Journal of King Saud University – Computer and Information Sciences

journal homepage: www.sciencedirect.com

A multi-layer hyper-graph routing with jamming-awareness for improved throughput in full-duplex cognitive radio networks

Sharhabeel H. Alnabelsi [a,b,*], Haythem Bany Salameh [b,c], Ramzi R. Saifan [d], Khalid A. Darabkh [d]

[a] Computer Eng. Dept., Faculty of Eng. Technology, Al-Balqa Applied University, Amman, Jordan
[b] College of Engineering, Al Ain University, Al Ain, United Arab Emirates
[c] Department of Telecommunication Engineering, Yarmouk University, Irbid 21163, Jordan
[d] Computer Eng. Dept., The University of Jordan, Jordan

A R T I C L E I N F O

Article history:
Received 21 September 2021
Revised 13 December 2021
Accepted 5 January 2022
Available online xxxx

Keywords:
Primary users
Secondary users
Jamming
Awareness
Full-duplex
Time sharing
Data rate
Throughput
Cognitive radio

A B S T R A C T

There are differences between routing in traditional and in Cognitive Radio Networks (CRNs). The availability of channels, periodic spectrum sensing, jammers activity, are some of these differences, etc. CRNs may contain a large number of Internet of Things (IoT) devices, hence, modeling such networks with a flat graph model generates a huge graph size. Thus, the motivation behind this work is clear bearing in mind that modeling such networks with a Multi-layer Hyper-Graph (MLHG) is the idea presented in this paper, in which each hyper-edge represents a group of CR devices, and each layer represents a licensed channel. In this paper, the main aim is to consider four key factors to maximize end-to-end network throughput, which are, transmission rate, licensed users activity, jammers activity, and needed number of time sharing. In literature, considering both jamming activity and time sharing for routing exists in few papers till now. This work proposes and develops three cutting-edge routing protocols that are aware of the four aforementioned factors, namely, Jamming-Activity-Sharing-Rate-Aware protocol, Jamming-Activity-Rate-Aware protocol, and Jamming-Activity-Sharing-Aware protocol. We compare these protocols with three recent proposed protocols in CRNs. Simulation results indicate that when jammers activity and time sharing are considered, network throughput is significantly enhanced. Specifically, our proposed jamming-aware protocols significantly outperform the existing three jamming-unaware protocols by up to 127%.

1. Introduction

The unlicensed wireless spectrum bands became over crowded, because of the huge number of wireless smart and Internet of Things (IoT) devices. Therefore, a new technology was proposed that allows to dynamically access the underutilized portions of the licensed spectrum. Namely, Cognitive Radio (CR) technology, which empowers the Secondary (or unlicensed) Users (SUs) to access idle channels in the licensed spectrum when their Primary (or authorized) Users (PUs) are not active. When utilizing the licensed channels, SUs are required to vacate them immediately when PUs become active. Moreover, SUs are required to periodically sense the licensed channels, in order to detect PUs' appearance. Furthermore, jamming attacks may exist in wireless networks, in such cases the jamming (or unwanted) signals increase the noise level over SUs' signals. If the noise level is above a given threshold, then the desired signals cannot be recovered at the receiving side. As a result, SUs usually select the licensed channels that have the longest availability time, weakest level of jamming signals, and highest data rate, in order to enhance the end-to-end throughput.

Wireless networks require multi-hop communication, such as 5G networks that adopt the concept of device-to-device communications. Therefore, multi-hop routing should be investigated. However, in CR Networks (CRNs), multi-hop routing requires a special awareness of spectrum availability and management (Bayrakdar and Çalhan, 2018; Bayrakdar and Çalhan, 2017; Bany Salameh et al., 2016), jamming signals generated by attackers, and channels' achieved data rates. This is to enhance the selected route's life time and the achieved end-to-end throughput (Bany Salameh et al., 2020; Qureshi et al., 2016; Wei and Hu, 2018). Moreover, due to the nature of wireless communications, a malicious node may interrupt an ongoing transmission by starting to transmit over

* Corresponding author.
E-mail addresses: alnabsh1@bau.edu.jo, sharhabeel.alnabelsi@aau.ac.ae (S.H. Alnabelsi), haythem.banysalameh@aau.ac.ae (H. Bany Salameh), r.saifan@ju.edu.jo (R.R. Saifan), k.darabkeh@ju.edu.jo (K.A. Darabkh).

https://doi.org/10.1016/j.jksuci.2022.01.003
1319-1578/

the same channel at the same time, which causes signals corruption. These nodes are called jammers or attackers as they can conduct different types of jamming attacks and significantly degrade network's performance (Yousaf et al., 2017; Rajkarnikar et al., 2017; Bany Salameh and AL-Quraan, 2020).

Full-duplex (FD) technology allows wireless devices to transmit and receive at the same time either over the same channel (In-band FD (IB-FD)), or over different channels (Out-of-Band FD (OB-FD)). In this work, OB-FD is adopted due to its simplicity compared to IB-FD technology. Specifically, it has low hardware complexity as it does not require self-interference-cancellation techniques. In nature, wireless networks communications are based on multi-hop routing. Unfortunately, most of the existing multi-hop CRN routing protocols are based on Half-duplex (HD) technology, where users can only transmit or receive at a given time. Therefore, researchers have recently emerged FD technology in CR multi-hop routing, to maximize end-to-end throughput. However, in CRNs, channel assignment for HD multi-hop routing is not applicable in FD multi-hop routing. Recently, FD-based transmission in CRNs is investigated in Amjad and Akhtar (2017), where a huge improvement in spectrum efficiency was reported (Darabkh et al., 2019; Bany Salameh et al., 2020; Bany Salameh, 2020). In Sarret and Berardinelli (2016), Hua et al. (2019), and Bany Salameh and El-Khatib (2018), it is demonstrated that the FD provided almost double throughput compared to HD technology. Moreover, several routing approaches were proposed in literature for FD multi-hop routing. However, they are NP-hard and were relaxed to find approximate solutions with the worst-case complexity that is still exponential with the number of hops and channels.

1.1. Motivation

Most recent work considers wireless networks when number of devices is not large. To the best of our knowledge, there are no studies that consider large number of devices as in IoT networks. Thus, it is essential to investigate FD-CR multi-hop routing in large scale networks, however, it is very challenging task. Interestingly, this work develops low-complexity protocols for route selection and channel assignment. The aim is to find routes with the highest probability of successful transmission while considering the unique characteristics of multi-hop routing in CRNs. For example, a routing protocol must have awareness of PUs activity, jamming attacks, the bottleneck-data rate over the route, and the number of needed time shares for hops transmissions. Moreover, this work exploits the capabilities of FD technology when making routing decisions.

1.2. Contributions

The contributions of this work are summarized as follows:

- Proposing three routing protocols that are aware of jamming, primary users activity, bottleneck-data rate, and the number of needed time shares, namely, Jamming-Activity-Sharing-Rate-Aware (JASRA) protocol, Jamming-Activity-Rate-Aware (JARA) protocol, and Jamming-Activity-Sharing-Aware (JASA) protocol.
- Using FD transmission technology while making routing decisions, in order to maximize the achieved end-to-end throughput.
- Modelling a dense wireless network using multi-layer hypergraph (*MLHG*), in which a group of SUs in a square area is represented by a hyper-edge (*HE*). Thus, the computation complexity is reduced when finding the best route.
- Implicitly finding the channel assignment over each hop of the selected best route. That is because hops are located within the layers of the *MLHG*, where each layer models a specific licensed channel.
- Proposing routing protocols that have polynomial-time complexity in terms of number of nodes and edges. Unlike, the existing protocols that need optimization techniques with NP-hard time complexity, or sometimes relaxed problems that give approximate solutions.

1.3. Organization

This paper is organized as follows: Section 2 presents the literature review. Section 3 introduces some preliminaries about HD and FD communication technologies. Section 4 presents the proposed network model, the proposed CRN modelling using *MLHG*, and the probability of successful transmission analysis. Section 5 demonstrates our proposed three routing protocols. Section 6 presents the performance evaluation. Finally, Section 7 presents the conclusions.

2. Literature review

Dynamic spectrum access technology allows SUs to access the licensed channels. This is done under many conditions such as sensing requirement, immediate transmission termination when the PU becomes active, and a proper channels' selection strategy in terms of idle time, etc (Hassan et al., 2017). Moreover, as any wireless network, CR networks may suffer from jamming attacks (Bany Salameh et al., 2018; Shi and Sagduyu, 2018; Furqan et al., 2020; Hanawal et al., 2019; Gecgel et al., 2019; Bany Salameh and Otoum, 2020), therefore, jamming awareness by SUs is indeed another requirement. Thus, developing routing protocols a very challenging task. Many researchers proposed multicast routing protocols that consider these requirements when utilizing the licensed spectrum. For example, the multicast routing protocols that construct routing tree with an immunity to the frequent channel-links' failures were studied in Almasaeid et al. (2019). Plus, authors of Bany Salameh and Abusamra (2021) proposed a probabilistic-intelligent method for multicast routing in CR-multimedia networks. A cross-layer approach for joint multicast routes discovery, call-admission control, and channel assignment for CR wireless mesh networks were proposed in Aghaei and Avokh (2020). Moreover, multicast routing with energy optimization was investigated in Kadhim and Seno (2019). A multicast routing protocol that is based on *MLHG* was proposed in Alnabelsi and Kamal (2013), in which the multicast routing session was found based on reducing both the number of routing failures and the end-to-end delay. Furthermore, the *MLHG* is utilized in Alnabelsi (2017), in order to find a primary and a protection path. The primary path is protected against PU activity, while the protection path is vulnerable to failures due to PU activity.

Note that the aforementioned routing protocols were based on HD transmission adopted by the SU nodes along the route. Clearly, an SU cannot transmit and receive at the same time neither over the same channel nor over different channels. Hence, the number of required time shares along the path gets increased. As a result, these routing protocols cannot be used when FD transmission technique is adopted by SUs.

To the best of our knowledge, routing in CRN along with FD transmission is recently studied only by few researchers, as follows. In Bany Salameh and El-Khatib (2018), a model was developed to generate channel assignment over a selected route such that the number of used channels is minimized, the throughput is maximized. Also, authors in Darabkh and Amro (2020) developed a simulator for in-band FD CRNs for internet of things environment, in which the achieved throughput was measured against many factors. Some of them are channel's availability, number of channels, monitoring cycle time for channels, SUs transmission range, etc. In-band-FD technology in CR ad hoc network was investigated in Darabkh et al. (2020), in which two routing protocols were proposed, without the need for common control channel, and the throughput was their objective. Moreover, authors in Bany Salameh et al. (2020) proposed a routing selection protocol that gives channel assignment under FD-awareness. However, their goal was only to maximize the route's throughput. Also, another routing mechanism is proposed was Bany Salameh (2020) that amazingly considers the number of sharing times along the route. This protocol generates channel assignment along the path under FD-awareness. It is worth mentioning that their work is the first which introduces a quantified equation to find the required number of time shares (that is utilized in this work). However, this protocol aims only to reduce the number of time shares in order to maximize the effective throughput. The related work is summarized in Table 1.

3. Preliminaries

3.1. Routing throughput based on HD channel assignment

In HD technology, communicating devices can transmit or receive during a given time. However, they cannot transmit and receive at the same time due to their hardware limitation. Therefore, for HD routing, the intermediate nodes should receive data, store it, and then forward it to the next hop.

At this point, one can discuss the effect of channel assignment on E2E throughput for HD routing, by taking the following example: given the route in Fig. 1, if hop 1 and hop 2 are assigned to either the same channel or different channels, B cannot transmit and receive at the same time due to its limited HD capabilities. However, C can transmit to D at the same time only if it uses a different channel from the one used for hop 1, in order to avoid interference to B reception. In other words, transmissions $A \rightarrow B$ and $C \rightarrow D$ can occur simultaneously. However, transmissions $B \rightarrow C$ and $D \rightarrow E$ cannot proceed at the same time when the former two transmissions are active. That is because B and D are currently receiving data and cannot transmit at the same time. In general, for HD multi-hop routing, assigning different channels to transmitters that are two hops far from each other increases the throughput. On the other hand, assigning different channels to transmitters that are three-hops or more far from each other does not improve the throughput. For example, in Fig. 2, channel 1 (C1) is assigned for hops 1 and 2. Further, channel 2 (C2) is assigned for hops 3 and 4. Therefore, the maximum possible throughput is achieved in HD, because either hops 1 and 3 or hops 2 and 4 can be active at the same time. Note that if hop 3 is assigned to channel 1, then, hops 1 and 3 cannot be active simultaneously, recall due to interference.

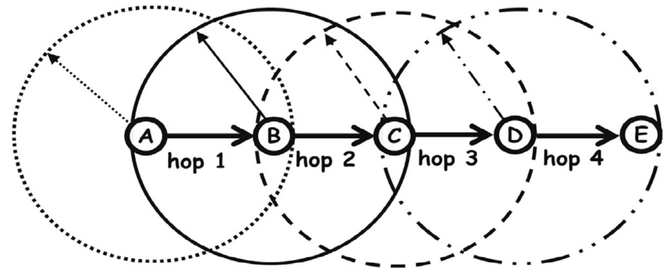

Fig. 1. instance of a route that consists four hops.

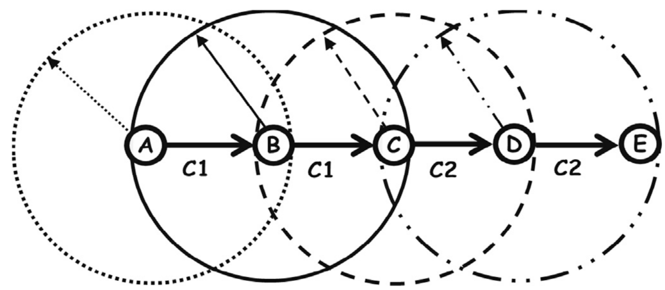

Fig. 2. Channel assignment for HD routing for maximum achievable throughput.

3.2. Routing throughput based on FD channel assignment

FD technology allows a device to transmit and receive at the same time. Since this work adopts OB-FD, then one can consider the route shown in Fig. 1, where all nodes have FD capabilities. In this case, B can receive from A (hop 1) and can transmit to C (hop 2) simultaneously if-and-only-if distinct channels were used to avoid self-interference. Moreover, C can proceed with transmission to D at the same time if-and-only-if it uses different channels from the ones used for hops 1 and 2. This is to avoid self-interference at C and the interference at B.

In other words, these transmissions $A \rightarrow B, B \rightarrow C$, and $C \rightarrow D$ can be active at the same time, when distinct channels are assigned to each hop (i.e.; three distinct channels are used). On the other hand, for hop 4 it is not necessary to assign a channel different from hop 1, because its nodes' transmission ranges do not overlap with B reception range. Apparently, hop 4 channel must be different from the previous two hops' selected channels. In general, it is concluded that for every three-consecutive hops, each must be assigned a distinct channel in order to have concurrent transmissions. This is to say that for a given multi-hop route, if the aforementioned condition holds, then none of the nodes store data, hence, the effective throughput is the bottleneck-data rate. Fig. 3 illustrates an example for channel assignment of OB-FD routing, where all hops transmissions can be active simultaneously.

Table 1
Literature review summary.

References	Full-duplex	Jamming aware	Polynomial time	Hyper-graph
Almasaeid et al. (2019), Bany Salameh and Abusamra (2021), Aghaei and Avokh (2020), Kadhim and Seno (2019)	No	No	No	No
Alnabelsi and Kamal (2013)	No	No	No	Yes
Alnabelsi (2017)	No	No	Yes	Yes
Bany Salameh et al. (2020), Bany Salameh (2020), Bany Salameh and El-Khatib (2018), Darabkh and Amro (2020), Darabkh et al. (2020)	Yes	No	No	No

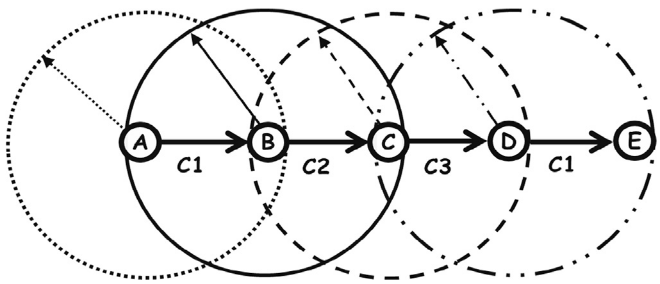

Fig. 3. Channel assignment for FD routing for maximum achievable throughput (all hops are activated simultaneously).

3.3. Illustrative example

To illustrate this work's motivation for using OB-FD technology while minimizing the number of time shares, one can assume a CRN consisting of 10 SUs, and 3 licensed channels. Furthermore, three paths are discovered, namely, P_1, P_2, and P_3, as shown in Fig. 4. For these paths, the selected channels and achieved data rate for each channel's link are assumed as they appear in this figure.

Definition 1 (*Time sharing*). It means one or more SUs are allowed to transmit at the same time instance, such that their concurrent transmissions do not interfere with each other. This time instance is counted as one-time share.

For example, for P_1 in Fig. 4, hops $1, 2$, and 4 can transmit at the same time, because there is no caused interference. However, hop 3 cannot be active when hop 1 is active, because they use the same channel (C_1). Consequently, in order to deliver one packet from SU1 to SU6, one extra-time share is needed ($NT_S = 1$), thus, totally two time shares are required. On the other hand, for P_3, all hops can be active at the same time, because there is no caused interference. Hence, one time share is needed (no extra-time share is required, $NT_S = 0$) to deliver the packet from SU1 to SU6.

To find the maximum achievable data rate for each path, one can identify the hop with the minimum data rate along the path and divide it by the number of needed time shares, as follows:

1. Path 1: hop 3 has the minimum data rate, therefore, the bottleneck-data rate is 6 Mbps. To find the number of needed time shares, one extra-time sharing is needed. This means $NT_S = 1$, and thus, the maximum achievable data rate for this path is $\frac{6}{NT_s+1} = \frac{6}{1+1} = 3$ Mbps.
2. Path 2: hop 2 has the minimum data rate, which means the bottleneck-data rate is 8 Mbps. The number of needed time shares is three as hops 1 and 3, hops 2 and 4, and hops 3 and 5 use the same channel, $NT_S = 3$, and the maximum achievable data rate for this path is $\frac{8}{NT_s+1} = \frac{8}{3+1} = 2$ Mbps.
3. Path 3: hop 4 has the minimum data rate with bottleneck-data rate as 4 Mbps. One can find the number of needed extra-time shares by considering that hops 1 and 3, hops 2 and 4, and hops 3 and 5 use different channels, thus, no extra time shares are needed. As a result, $NT_S = 0$, and therefore, the maximum achievable data rate for this path is $\frac{4}{NT_s+1} = \frac{4}{0+1} = 4$ Mbps.

Apparently, adopting the shortest path for routing, such as P_1, is not necessarily the best path in terms of effective throughput. Further, selecting the path that has the maximum bottleneck-data rate, such as P_2, is also not necessarily the best path. That is because of the time sharing effect which can significantly decrease the network's throughput. When the number of required time shares is considered, P_3 actually has the maximum data rate. Therefore, this work considers the number of required time shares along with the achieved data rate in its proposed routing algorithms. It is worth pointing out that for OB-FD technology, a quantified impact of extra-time shares, NT_s, for a given path was recently introduced in Bany Salameh (2020) and computed as follows;

$$NT_S(p) = (K_p - 2) - \frac{1}{2}\sum_{i=1}^{C}\sum_{j=1}^{K_p-2}\left(x_{p,j}^{(i)} - x_{p,j+2}^{(i)}\right)^2 \quad (1)$$

In the above expression, p denotes a path, K_p represents the number of hops over the path, C denotes the number of channels, $x_{p,j}^{(i)}$ is a binary variable that is equal to 1 if channel i is used over hop j of path p. Otherwise, it is zero (i.e.; $x_{p,j}^{(i)}$ represents the channel assignment).

4. Network model and hyper-graph model

This work considers an ad hoc wireless CRN that coexists with a licensed network, e.g.; cellular network. The CRN operates in the presence of jammers, as illustrated in Fig. 5. (a). The licensed network includes a cellular network service provider and PUs (client devices). We consider a proactive jamming, where the inter-arrival times of jamming and the inter-arrivals times of PU are independent and follow exponential distribution. The set of SUs exchange control information, e.g.; channels availability, using the established common-control channel (Thilina, 2015; Miazi and Tabassum, 2015; Cicioğlu et al., 2019). The source and the destination SU nodes can be any two SUs from the set $\mathcal{S} = \{1, 2, \ldots, S\}$, where S is the total number of SUs that can establish links in an ad hoc manner. Assume SUs opportunistically access a set of licensed channels, say $\mathcal{C} = \{1, 2, \ldots, C\}$, where C is the total number of licensed channels. Moreover, SUs have FD transmission capabilities. It is assumed that the self-interference can be significantly mitigated using recent self-interference cancellation (SIC) techniques (e.g., digital SIC techniques Ahmed and

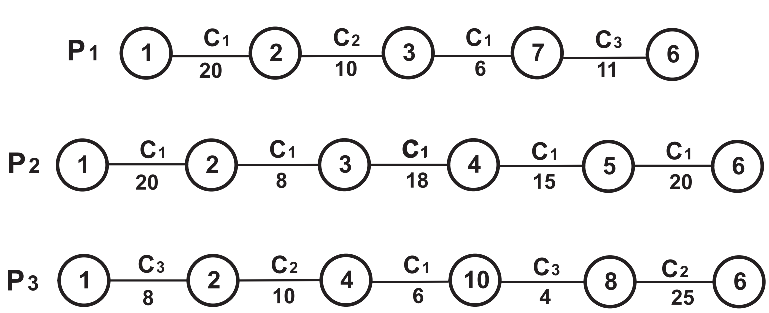

Fig. 4. Motivation example to demonstrate time sharing effect in full-duplex transmission.

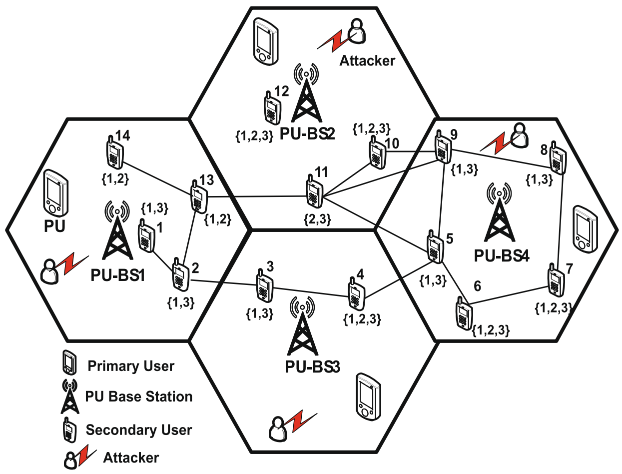

(a) CRN and primary cellular network.

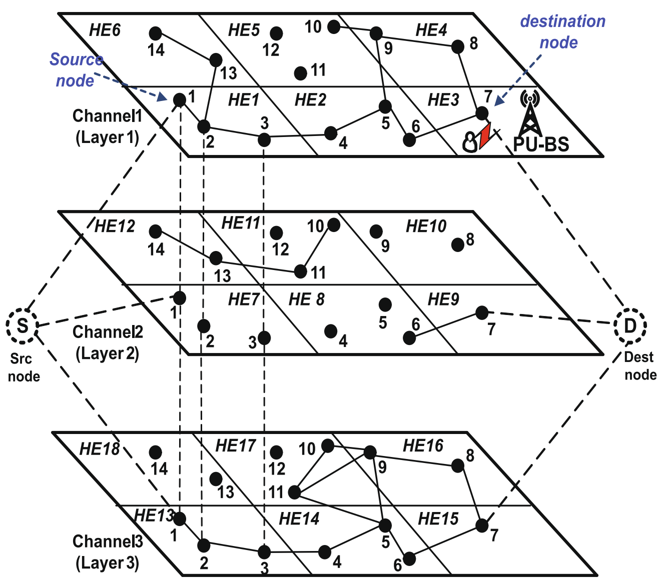

(b) CRN modelling as a $MLHG$.

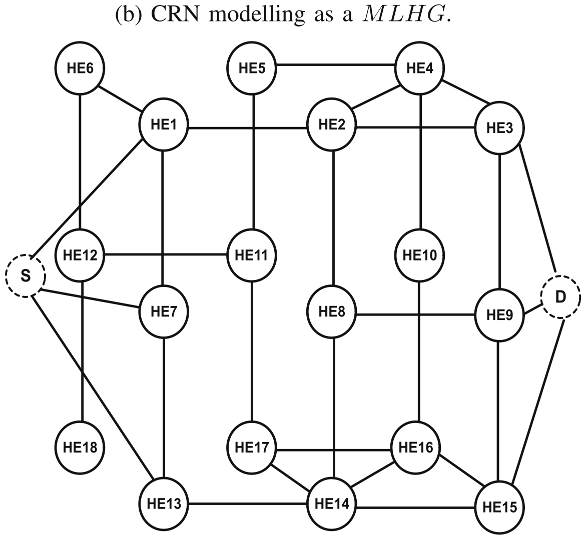

(c) The conversion of the $MLHG$ to a simple graph.

Fig. 5. The motivation example for best route selection in CRN under jamming attacks.

Eltawil, 2015). In addition, the work in Bharadia et al. (2013) demonstrated that the self-interference can be significantly reduced in FD systems by up to 110 dB. This results in negligible impact of the residual self-interference on system performance, making the FD communication practically feasible. In this paper, we focus on the problem of spectrum assignment and route selection assuming that the SIC techniques implemented in Bharadia et al. (2013) and Nguyen and Tran (2020) are in place, which reduce the residual self-interference to the noise floor. The used notions and their descriptions are introduced in Table 2.

4.1. The proposed multi-layer hyper-graph network model

CRNs nature allows an SU to find multiple channels available over one link, hence, this cannot be modeled using simple graphs. This point shows the motivation behind this work to model CRNs using *MLHG* (Mikko and Arenas, 2014; Boccaletti and Ginestra, 2014; McGee and Ghoniem, 2019). The *MLHG* contains a set of layers, where each layer contains a set of hyper-edges (*HEs*), the *HE* may have more than two vertices, unlike simple edges in traditional graphs. *MLHG* allows designers to capture the fact that at any link multiple channels can be available. Thus, in the proposed model, each layer in the graph represents one channel. Moreover, the vertices in an *HE* represents SU nodes.

In the proposed model, a flat area of SUs, such as the CRN shown in Fig. 5. (a), is divided into a set of equal-sized square areas in order to reduce the computation complexity. Interestingly, each square area and its corresponding SUs are replicated in every layer. Moreover, each square area is modeled as an *HE* in the *MLHG*. Note that SUs in the same square area are within the transmission range of each other.

Definition 2 (*Layer*). A licensed channel is modeled as a layer in the *MLHG*.

Definition 3 (*Hyper-edge*). A square area that consists of some SUs in a layer is modeled as a *HE*.

Definition 4 (*Vertical-dashed line*). It exists between two consecutive layers in the *MLHG* and represents switching between two channels for an SU transceiver.

Fig. 5. (b) shows that each square is replicated in all layers. For example, square 1 (HE_1), square 7 (HE_7), and square 13 (HE_{13}) are the replication for one square area in the flat CRN. Moreover, when an SU is replicated in each layer, a vertical-edge connects every two replications in two consecutive layers to model layers' (channels') switching. In our model, when a route is found for the *MLHG*, the channel assignment is implicitly found. For example, when a selected route switches from the current layer, say layer *i*, to another layer, say layer *j*, then an SU along this route has switched its transceiver from channel *i* to channel *j*. Consequently, route discovery and its channel assignment require a polynomial-time complexity, as this is one of this work's major contributions. After constructing the *MLHG* as in Fig. 5. (b), it can be converted to a simple graph, as shown in Fig. 5. (c). This is needed when applying route discovery protocols which are suitable for simple graphs. The conversion steps will be explained later in this section. The illustrative example in Fig. 5. (a) contains four PUs' base stations, a set of jamming attackers, a set of PUs, and a group of 14 SUs. Assume at a certain time, for the purpose of the route discovery, the source node is SU1 and the destination node is SU7, the available channels for each SU are shown beside it. For example, SU1 has channels 1 and 3 available in cell 1 of the base station for PU1, labeled as PU-BS1. The available connectivity links between

Table 2
Notations.

Symbol	Description	Symbol	Description
CR	cognitive radio	CRN	cognitive radio network
SU	Secondary user	PU	Primary user
s	source-SU node	d	destination-SU node
$\mathscr{S}$	the set of SUs in the network	$\mathscr{C}$	the set of licensed channels in the network
G	network graph of a CRN that contains a set of SUs.	HG	hyper-graph.
HE	a hyper-edge that belongs to $\mathscr{HE}$ set.	$\mathscr{HE}$	the set of hyper-edges that constructs the HG.
$MLHG$	multi-layer hyper-graph.	$e(i,j)$	an edge between SUi and SUj in G graph.
$\mathscr{E}$	the set of edges that constructs G.	$\mathscr{E}\prime_{(i,j)}$	the set of SUs' edges that connects HE_i and HE_j.
$HL^p(i,j)$	a hyper-link along path p that represents a communication link between the adjacent HE_i and HE_j either horizontally or vertically.	$\mathscr{HL}$	the set of hyper-links that connect the hyper-edges in a given $MLHG$.
$\mathscr{HL}^p$	the set of hyper-links that constructs the hops of path p.	HLG	hyper-link graph that constructed using the set of $\mathscr{HL}$ as edges and the set of $\mathscr{HE}$ as vertices.
$\mathscr{P}$	the set of found k-shortest paths in HLG from a HE that contains the source SU to the HE that contains the destination SU.	p	one of the shortest paths, $p \in \mathscr{P}$.
$\overline{T}^{(i)}_{ava}$	the average availability time, i.e. the average inter-arrival time for PU's transmission; for channel i.	$\overline{T}^{(i)}_{jam}$	the average jamming time, i.e.; the average inter-arrival time for channel i.
$\overline{T}^{(i,j)}_{ava}$	the average availability time for channel i over HE_j.	$\overline{T}^{(i,j)}_{jam}$	the average jamming time for channel i over HE_j.
HD	Half-duplex.	$c(i)$	the index of the licensed channel for HE_i
$R^{(i,j)}_{c(i)}$	is the data rate over channel $c(i)$ for the HL that connects HE_i and HE_j at the same hyper-graph layer where $c(i) = c(j)$	PoS	probability of success.
$PoS^a_{(i,c(i))}$	probability of successful transmission with awareness about jamming for a SU that resides in HE_i over channel $c(i)$.	$PoS^u_{(i,c(i))}$	probability of successful transmission without awareness about jamming for a SU that resides in HE_i over channel $c(i)$.
$PoS^a_{e(i,j)}$	probability of successful transmission, with awareness about jamming, between SUi and SUj.	$PoS^u_{e(i,j)}$	probability of successful transmission, without awareness about jamming, between SUi and SUj.
$PoS^{a,max}_{HL^p(i,j)}$	the maximum probability of successful transmission between all existing SUs links that connects HE_i and HE_j for path p, where SUs are aware about jamming.	$PoS^{u,max}_{HL^p(i,j)}$	the maximum probability of successful transmission between all existing SUs links that connects HE_i and HE_j for path p, where SUs are unaware about jamming.
$t^{c(i)}_x$	is the required transmission time over the channel of HE_i.	$NT_s(p)$	number of extra-time sharing that required for transmission a long path p.
$R^{HL(i,j)}_{eff}$	the effective data rate for the HL that connects HE_i and HE_j at the same hyper-graph layer where $c(i) = c(j)$.	R^p_{bott}	the bottleneck-effective data rate for path p.
p^*	the index of the shortest path that has the maximum R^p_{bott} between the found k-shortest path, $\mathscr{P}$.	FD	Full-duplex

SUs are also illustrated in this figure, for instance SU2 can communicate with SU3 over the common-available channels 1 and 3. Establishing a link between two SUs depends on common channels' availability, transmission distance, and channels' quality.

4.2. Flat network conversion to MLHG

To convert a flat network such as the CRN illustrated in Fig. 5. (a) to a *MLHG* as shown in Fig. 5. (b), the following assumptions and steps are applied;

Assumptions:

1. Channels availability is relatively sustained for a long time. Some licensed channels, such as TV channels (54 MHz–862 MHz), have availability times that are longer compared to other licensed channels with high PUs' activity (IEEE, 2011).
2. SUs located in the same *HE* (square) are affected by the same PU's interference range and the same jamming range of the attacker.
3. Although some SUs have a close distance, they may not be able to communicate with each other over some channels. That is due to bad channels' conditions, e.g.; noise, fading.

Steps:

1. A dummy-source node, s, is introduced to be connected with the SU-source node which is replicated in all layers, as the dashed-edges shown in Fig. 5. (b).
2. A dummy-destination node, d, is introduced in order to connect it with the SU-destination node which is replicated in all layers, as the dashed-edges shown in Fig. 5. (b).
3. In each layer all SU nodes are replicated, a link between two SUs in one layer, say layer 2, implies that these two SUs can communicate over channel 2. Otherwise, these two SUs cannot communicate over channel 2.
4. When a layer is divided into squares (*HEs*), some SUs' links become located in two adjacent squares.
5. The vertical-dashed lines between any two layers, shown in Fig. 5. (b), denote channels' switching by SUs. For example, the vertical-dashed line between layer 1 and layer 2 for SU1 represents SU1 switching its transceiver from channel 1 to channel 2 or vice versa. Another example, consider the vertical-dashed line between layers 2 and 3 for SU1, this line represents the ability of SU1 transceiver to switch from channel 2 to channel 3 or vice versa. Moreover, the vertical-dashed line between layers 1 and 3 for SU1 represents SU1 switching its transceiver from channel 1 to 3 or vice versa. Note that the SU switches to another channel only when it is idle. For illustration, vertical-dashed lines are drawn only for SU1, SU2, and SU3. However, the vertical-edges exist for all SUs between different layers.

In summary, the CRN shown in Fig. 5. (a) is transformed to an *MLHG* as shown in Fig. 5. (b), such that each layer represents a licensed channel, each *HE* represents a square area that has some SUs, and each vertical-dashed line represents channels' switching.

In this figure, there are 6 squares in each layer, and hence, totally there are 18 *HEs* and 28 vertical-dashed lines between these layers.

4.3. MLHG conversion to simple hyper-link graph

In order to transform the constructed *MLHG*, shown in Fig. 5. (b), into a simple graph, namely Hyper-link Graph (*HLG*), shown in Fig. 5. (c). The *HLG* consists of a set of vertices and a set of edges (these edges are named Hyper-links (*HLs*)). Specifically, the set of vertices in *HLG* represents the set of $\mathscr{HE}$ in the *MLHG*, and the set of edges in *HLG* denotes the set of $\mathscr{HL}$ that is extracted from the *MLHG*, as will be explained later in this subsection. The Hyper-link (*HL*) can be horizontal or vertical when extracted from the *MLHG*, however, there are some differences between them and they can be defined as follows;

Definition 5 (*Vertical Hyper-link*). It exists between two consecutive layers in the *MLHG* which connects two *HEs* when at least one vertical-dashed line exists between the two *HEs*.

Definition 6 (*Horizontal Hyper-link*). It exists between two adjacent *HEs* in the *MLHG* when there is at least one edge established between a pair of SUs for data communication, such that each SU is located in different *HE*.

In other words, the horizontal *HL* denotes the data communication over the same channel, while vertical *HL* denotes channels switching between two channels for a SU. Note that this proposed graph model is general, thus, one can have some notes as follows;

- Although SU14 does not have channel 3 available, a vertical-edge between HE_{12} and HE_{18} exists. However, when a route discovery method is applied and it reached to HE_{18} node, as shown in Fig. 5. (c), then this node is a leaf node. Hence, the discovery process gets terminated at this node and continued with other nodes.
- Although an *HE* does not have SUs with established communication links, it still gets represented in the *HLG* such as node 10 (which represents HE_{10}) in Fig. 5. (c). Apparently, this node does not have horizontal *HLs*, however, it has vertical *HLs* which implies the possibility for a route segment to go from node 4 to node 16 or vice versa. Meaning, this segment implies that one of the SUs (SU8 and SU9) located in the corresponding square area has switched its transceiver from channel 1 to channel 3 or vice versa. Recall, this square area is replicated as HE_4, HE_{10}, and HE_{16}.

The steps for converting the *MLHG* to *HLG* are as follows;

1. A *HL* exists between two square areas (two *HEs*), if-and-only-if there is at least one SUs' edge between them. For example, in layer 1, shown in Fig. 5. (b), edge $e(3,4)$ is the only edge that exists between HE_1 and HE_2, thus, this edge is selected as the *HL* between these two *HEs*. Another example, $HL(8,9)$ shown in Fig. 5. (c) represents the communication link between SU6 and SU7 in layer 2, as shown in Fig. 5. (b).
2. Sometimes at the same layer, two adjacent squares may have more than one common SUs' edges. For example, HE_{16} and HE_{17} have two common edges, namely $e(9,10)$ and $e(9,11)$, the edge with the highest probability of successful transmission is selected as a horizontal *HL*, namely $HL(16,17)$, between these two adjacent *HEs*. Notice that $HL(16,17)$ is actually the edge between nodes HE_{16} and HE_{17}, as shown in Fig. 5. (c).
3. At any two consecutive layers, vertical *HLs* exist between the replicated square areas (*HEs*) if-and-only-if at least one SU is located in the square area. For example, for layer 1 and layer 2, the vertical *HLs* are $HL(1,7), HL(2,8), HL(3,9), HL(4,10)$, $HL(5,11)$, and $HL(6,12)$, as illustrated in Fig. 5. (c).

Later, when we discuss the Probability of Success (PoS) for these vertical *HLs*, each one has a PoS that is equal to 1 because the SU's transceiver can switch between channels when needed. Also, the PoS is set to 1 for the introduced dashed-edges in the *MLHG* which connect the dummy nodes, *s* and *d*. On the contrary, the probability of successful transmission between two SUs that is denoted by horizontal *HLs* will be different and is discussed in the following subsection.

4.4. The probability of success analysis

In general, when jammers exist in a CRN, the packet's transmission time must be less than or equal to the channel's availability time, and less than or equal to the jammers idle time. In other words, for a successful packet transmission at a given licensed channel, its transmission time must be less than or equal to the inter-arrival time for the jammer and the inter-arrival time of the PU. For a flat CRN, a closed-form expression for the probability of successful transmission between any two communicating SUs over a given channel, say channel *i*, has been derived as follows: $\exp\left(-t_x \frac{\overline{T}^{(i)}_{ava}+\overline{T}^{(i)}_{jam}}{\overline{T}^{(i)}_{ava}\overline{T}^{(i)}_{jam}}\right)$, where t_x is the transmission time (Bany Salameh and Otoum, 2020). In our work, we assume the SUs pair, say SU*i* and SU*j*, are located in different-adjacent square areas, say area *k* (denoted by HE_k) and area *m* (denoted by HE_m) with the existence of independent PU and jammer. Hence, the POS transmission is computed as follows;

$$PoS^a_{e(i,j)} = \begin{cases} PoS^a_{(k,c(k))}PoS^a_{(m,c(m))} = \left(\exp\left(-Z_a(k)\right).\exp\left(-Z_j(k)\right)\right)\left(\exp\left(-Z_a(m)\right).\exp\left(-Z_j(m)\right)\right) \\ \qquad = \exp\left(-Z_a(k)-Z_j(k)\right).\exp\left(-Z_a(m)-Z_j(m)\right) \\ \qquad ;\text{if} c(k)=c(m); e(i,j)\in \mathscr{E}\prime_{(k,m)}; c(n)\in\mathscr{C}, \forall n\in\mathscr{HE}. \\ 1 \qquad ;\text{if} c(k)\neq c(m); e(i,j)\in \mathscr{E}\prime_{(k,m)}; c(n)\in\mathscr{C}, \forall n\in\mathscr{HE}. \end{cases} \tag{2}$$

where $Z_a(k)=\left(\frac{t_x^{c(k)}}{\overline{T}^{(c(k),k)}_{ava}}\right)$; $Z_j(k)=\left(\frac{t_x^{c(k)}}{\overline{T}^{(c(k),k)}_{jam}}\right)$; $Z_a(m)=\left(\frac{t_x^{c(m)}}{\overline{T}^{(c(m),m)}_{ava}}\right)$; $Z_j(m)=\left(\frac{t_x^{c(m)}}{\overline{T}^{(c(m),m)}_{jam}}\right)$;

$\left(-Z_a(k)-Z_j(k)\right)=-t_x^{c(k)}\frac{\overline{T}^{(c(k),k)}_{ava}+\overline{T}^{(c(k),k)}_{jam}}{\overline{T}^{(c(k),k)}_{ava}\overline{T}^{(c(k),k)}_{jam}}$; $\left(-Z_a(m)-Z_j(m)\right)=-t_x^{c(m)}\frac{\overline{T}^{(c(m),m)}_{ava}+\overline{T}^{(c(m),m)}_{jam}}{\overline{T}^{(c(m),m)}_{ava}\overline{T}^{(c(m),m)}_{jam}}$.

Noting that the set of SUs edges that are common between two adjacent *HEs*, say HE_k and HE_m, are denoted by $\mathscr{E}\prime_{(k,m)}$, where $\mathscr{E}\prime_{(k,m)}\subseteq\mathscr{E}$. Also, in Eq. (2), the PoS is set to one for all vertical *HLs*, because SU's transceiver can switch between channels when needed. Recall that, the vertical *HL* connects two different layers that mapped to different channels.

In Eq. (2), when the square areas are homogeneous in terms of average availability and jamming times, i.e.; they are equal for all square areas for a given channel, this equation is reduced as follows;

$$PoS^a_{e(i,j)} = \begin{cases} \exp\left(-2Z_a(k)-2Z_j(k)\right);\ \text{if} c(k)=c(m);\ e(i,j)\in \mathscr{E}\prime_{(k,m)}; c(n)\in\mathscr{C}, \forall n\in\mathscr{HE}. \\ 1 \qquad ;\text{if } c(k)\neq c(m); e(i,j)\in \mathscr{E}\prime_{(k,m)}; c(n)\in\mathscr{C}, \forall n\in\mathscr{HE}. \end{cases} \tag{3}$$

On the other hand, the SUs may not be aware of jamming existence, but, they are aware of channels' average availability (i.e., PU activity). In this case, an SU's packet transmission is successful, at a given licensed channel, if its required transmission time is less than or equal to this channels' average availability time. Generally, in a flat CRN, an equation has been derived in order to find probability of successful transmission between any two communicating SUs as follows: $\exp\left(-\frac{t_x}{\overline{T}^{(i)}_{ava}}\right)$ (Badarneh and Bany Salameh, 2011).

However, we modified this equation to be suitable for our proposed network model, assuming that the communicating SUs, say SU*i* and SU*j*, are located in HE_k and HE_m, respectively, as follows:

$$PoS^u_{e(i,j)} = \begin{cases} PoS^u_{(k,c(k))}.PoS^u_{(m,c(m))} = \exp(-Z_a(k)).\exp(-Z_a(m)); \text{if} c(k) = c(m); e(i,j) \in \mathscr{E}\prime_{(k,m)}; \\ \qquad c(n) \in \mathscr{C}, \forall n \in \mathscr{HE}. \\ 1 \qquad ; \text{if } c(k) \neq c(m); e(i,j) \in \mathscr{E}\prime_{(k,m)}; c(n) \in \mathscr{C}, \forall n \in \mathscr{HE}. \end{cases} \quad (4)$$

Similarly, for Eq. (4), when the square areas are homogeneous in terms of average availability time, i.e.; they are equal for all square areas of a given channel, this equation is reduced as follow;

$$PoS^u_{e(i,j)} = \begin{cases} \exp(-2Z_a(k)); \text{ if } c(k) = c(m); e(i,j) \in \mathscr{E}\prime_{(k,m)}; c(n) \in \mathscr{C}, \forall n \in \mathscr{HE}. \\ 1 \qquad ; \text{if } c(k) \neq c(m); e(i,j) \in \mathscr{E}\prime_{(k,m)}; c(n) \in \mathscr{C}, \forall n \in \mathscr{HE}. \end{cases} \quad (5)$$

It is well known that finding the required transmission time for a packet, $t^{(c)}_x$, over a given channel, say channel *c*, depends on the packet size, *D*, and the channel's rate, $R^{(c)}$, where $t^{(c)}_x = \frac{D}{R^{(c)}}$. The channel's rate follows Shannon–Hartley's theorem that is subject to Additive white Gaussian Noise (AWGN), $R^{(c)} = BLog_2\left(1 + SNR^{(c)}\right)$, where *B* and *SNR* denote the channel bandwidth and signal-to-noise ratio, respectively. $SNR^{(c)} = \frac{p^{(c)}_r}{N_o}$, such that $p^{(c)}_r$ and N_o denote the received power and noise density, respectively. $p^{(c)}_r = \alpha \frac{p^{(c)}_t}{d^n}\Gamma$, such that $p^{(c)}_t$ represents the transmission power, Γ is an exponential random variable with a mean equals to $1, d$ denotes distance, *n* denotes path loss exponent, $\alpha = \left(\frac{G_t G_r}{\lambda}\right)^2$, where G_t and G_r are the gain at the transmitter and the receiver, respectively, and $\lambda = \frac{L_s}{f}, L_s$ is the light speed and *f* is the signal frequency.

It can be noted that in some cases there are more than one candidate edges between two adjacent *HEs*, such as in Fig. 5. (c) between HE_{16} and HE_{17} in layer 3. In this proposed model, the edge with the maximum probability of successful transmission is selected as a *HL* between those two *HEs*. To explain this scenario in more details, consider another CRN example as shown in Fig. 6, in which an instance of two square areas (*HEs*), namely *HEi* and *HEj*, is illustrated. A group of eleven SUs, $\{SU1, \ldots, SU11\}$, are located within these two *HEs*. There are multiple common edges between them, namely, $e(4,8), e(5,8)$, and $e(6,7)$. Let the probability of successful transmission of these edges be $0.6, 0.7$ and 0.8, respectively. One of these candidate edges will be selected as the *HL* between *HEi* and *HEj*. Therefore, edge $e(6,7)$ is selected to denote $HL(i,j)$ with a PoS equals to 0.8. This methodology is employed between any two adjacent *HEs* in the *MLHG*, in order to find all $HLs, \mathscr{HL}$, that are used to construct the *HLG*. In general, for any two adjacent *HEs*, say HE_k and HE_m, along a path, *p*, there is one or multiple common SUs' edges denoted as $\mathscr{E}\prime_{(k,m)}$, where $\mathscr{E}\prime_{(k,m)} \subseteq \mathscr{E}$. The edge with the maximum probability of successful transmission is selected as the *HL*, namely $HL^p(k,m)$, and the corresponding probability of successful transmission for this edge is set for this *HL* and found using Eq. (6). However, if the SUs in the network are not aware of jammers activity, then Eq. (7) is used.

$$PoS^{a,max}_{HL^p(k,m)} = \max\left(PoS^a_{e(i,j)}\right); \ \forall e(i,j) \in \mathscr{E}\prime_{(k,m)}. \quad (6)$$

$$PoS^{u,max}_{HL^p(k,m)} = \max\left(PoS^u_{e(i,j)}\right); \ \forall e(i,j) \in \mathscr{E}\prime_{(k,m)}. \quad (7)$$

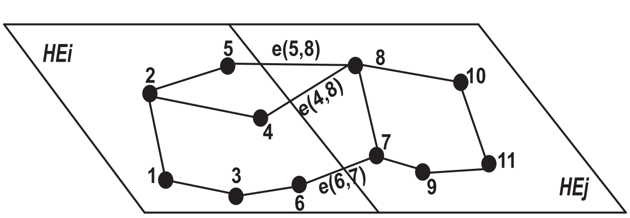

Fig. 6. An instance of two hyper-edges in a layer with multiple candidate links.

5. The proposed routing algorithms

This section introduces our proposed three algorithms, that are aware of jamming and channels' availability. Consequently, the SU's transmission is successful only when both the idle times of the corresponding channel's PU and the corresponding jammer are greater than or equal to the required SU's transmission time.

The proposed three routing algorithms consider some or all of the below listed key performance factors. Some of the proposed protocols do not consider all of those factors, this is done to asses the impact of the excluded factors on network's performance. These factors are as follows:

1. PUs activity: SUs consider the inter-arrival times for PU's packets.
2. Jammers' activity: SUs are aware about the inter-arrival times for jammers' interference.
3. Bottleneck-data rate (R^p_{bott}): the maximum achievable data rate along a path, *p*, depends on the bottleneck-data rate, which is defined as the rate of the link with the minimum data rate over the path.
4. Number of required extra-time shares (NT_s): recall, it is the number of extra times needed to deliver one packet from a source to a destination node, due to the caused interference between concurrent hops transmissions ($NT_s \geqslant 0$). This happens when FD transmission is adopted.

The proposed three routing protocols are presented in the next subsections, the considered graph when running these protocols is the *HLG* which is converted from *MLHG*, such as the graph in Fig. 5. (c). In this graph, assume that each *HL* has a unity cost, the initial step for any of the proposed protocols is to find the *k*-shortest paths, $\mathscr{P}$, such that any two selected shortest paths are different by at least one *HL*. After that, each candidate path is evaluated in order to find the best path in terms of the highest end-to-end throughput, this evaluation is based on the developed performance metrics of each protocol.

These proposed routing protocols have polynomial-time complexity, due to multiple reasons: first, the number of edges is reduced, because the network is divided into a set of square areas where each area is modeled as a *HE* in the *MLHG*. Second, the channel assignment is implicitly found, because each layer in the *MLHG* represents a channel. Third, the studied routes are found using a polynomial-time algorithm.

5.1. Jamming-activity-sharing-rate-aware (JASRA) protocol

This routing algorithm considers all four routing key factors that were discussed earlier. It considers jamming, PU's activity, number of needed time shares, and data rate. Clearly, this algorithm is expected to have high efficiency for the effective end-to-end throughput. For each path $p, p \in \mathscr{P}$, and each *HL* in *p*, the effective data rate is found by multiplying the data rate by the maximum probability of successful transmission, $PoS^{a,max}_{HL(i,j)}$, and the result is divided by number of time shares that were scheduled along the path, as;

$$R_{eff}^{HL^p(i,j)} = \frac{R_{c(i)}^{(i,j)} PoS_{HL^p(i,j)}^{a,max}}{NT_s(p)+1}; HL^p(i,j) \in \mathscr{HL}, PoS_{HL^p(i,j)}^{a,max} \neq 1 \tag{8}$$

In the next step, for each path, the minimum effective data rate for the hyper-links along the path is found as;

$$R_{bott}^p = \min R_{eff}^{HL^p(i,j)}; \; \forall HL^p(i,j) \in \mathscr{HL}^p, p \in \mathscr{P}. \tag{9}$$

In the last step, the path with the maximum bottleneck-data rate, R_{bott}^p, is selected for routing, as;

$$p^* = \arg\max_{p \in \mathscr{P}} R_{bott}^p. \tag{10}$$

The Pseudocode for this algorithm, JASRA, is illustrated in Algorithm 1.

5.2. Jamming-activity-rate-aware (JARA) protocol

In this protocol, the PoS is multiplied by the data rate in order to find the effective data rate for each *HL* within the evaluated path. However, it is not divided by number of time shares as in JASRA, i.e.;

$$R_{eff}^{HL^p(i,j)} = R_{c(i)}^{(i,j)} PoS_{HL^p(i,j)}^{a,max}; \; HL^p(i,j) \in \mathscr{HL}, PoS_{HL^p(i,j)}^{a,max} \neq 1 \tag{11}$$

Finding the bottleneck-data rate for a given path, R_{bott}^p, is also done using Eq. (9), and the index of the best route is found using Eq. (10). The Pseudocode of this algorithm (JARA) is the same as JASRA protocol that is illustrated in Algorithm 1, but, in line 3, Eq. (8) is replaced by Eq. (11).

5.3. Jamming-activity-sharing-aware (JASA) protocol

In this protocol, the effective data rate for each *HL* within the evaluated path is calculated by dividing the PoS by the number of required time shares over the path, as follows;

$$R_{eff}^{HL^p(i,j)} = \frac{PoS_{HL^p(i,j)}^{a,max}}{NT_s(p)+1}; \; HL^p(i,j) \in \mathscr{HL}, PoS_{HL^p(i,j)}^{a,max} \neq 1 \tag{12}$$

Finding the bottleneck-data rate for a given path, R_{bott}^p, is also done using Eq. (9), and the index of the best route is found using Eq. (10). The Pseudocode for this algorithm, JASA, is the same as JASRA protocol that is illustrated in Algorithm 1, however, in line 3, Eq. (8) is replaced by Eq. (12).

Algorithm 1: JASRA/JARA/JASA routing Algorithm

Input: $s, d, k, G(\mathscr{SU}, \mathscr{E}), HLG(\mathscr{HE}, \mathscr{HL}), t_x^{c(i)} \forall i \in \mathscr{HE}$, $\mathscr{C}, \overline{T}_{ava}^{(i,j)}, \overline{T}_{jam}^{(i,j)} \; \forall i \in \mathscr{C}, \forall j \in \mathscr{HE}$.
Output: $p^*, \mathscr{HL}^{p^*}, R_{bott}^{p^*}$
Initialization: find k-shortest paths in *HLG*, i.e.; all *HLs* for each found path, $\mathscr{HL}^p \in \mathscr{P}$.
1: **for** each path $p \in \mathscr{P}$ **do**
2: **for** each $HL(i,j) \in \mathscr{HL}^{\mathscr{P}}$ **do**
3: Find $R_{eff}^{HL(i,j)}$ using Eq. (8).
4: **end for**
5: For path p, find the bottleneck-data rate, R_{bott}^p, using Eq. (9).
6: **end for**
7: Find the index of the shortest path, p^*, that has the maximum bottleneck-data rate, using Eq. (10).

6. Performance evaluation

6.1. Simulation setup

MATLAB (Math Works, 2021) is used to conduct the simulation experiments, in order to assess a network performance in terms of the end-to-end effective throughput and number of successfully established paths. Different simulation parameters were investigated, including the probability of licensed channels being idle, number of licensed channels, jamming severity factor. Considering a CRN located in a network area of 500 m × 500 m. This network consists of 100 SUs, where each SU's transmission range is set to 100 m. When SU are deployed in the area, the minimum distance between any SUs pair is 5 m, to guarantee that SUs will be fairly deployed in the area. The channel's data rate is selected randomly between 40 Mbps and 80 Mbps in every simulation run (Shu et al., 2006). Data packet length is set to 2 KB. The number of employed channels, C, is set to 10. For these channels, the average channels' idle times (PUs packets inter-arrival times) and average jamming intervals follow independent exponential distribution random variables. Further, this work assumes the average idle times of these channels $\left(\overline{T}_{ava}^{(i)}, i = \{1, 2, \ldots, 10\}\right)$ to be $5, 100, 30, 5, 45, 50, 100, 5, 45$, and 30 ms. Plus, their average jamming intervals $\left(\overline{T}_{jam}^{(i)}, i = \{1, 2, \ldots, 10\}\right)$ are $5, 0.7, 5, 2, 10, 5, 1, 2.9, 20$, and $0.3 \times \Psi$ ms, where Ψ is an indicator of the jamming severity. Note that when Ψ becomes smaller (e.g.; 0.1), the inter-arrival times of jamming packets become smaller (i.e.; high jamming activity). On the other hand, when Ψ becomes larger (e.g.; 2), the inter-arrival times of jamming packets become larger (i.e.; Low jamming activity). In every simulation run, to find channels idle and jamming times, the aforementioned average intervals of channels are used to withdraw these values from their exponential distribution. Recall that, these values are used in determining whether the packet is successfully transmitted or not for every channel over every hop along the investigated paths. The k–shortest path algorithm is used to find the set of paths to be investigated. It is worth mentioning that all results are the average of 1000 runs, each with a different topology and channels' conditions. The simulation parameters are summarized in Table 3.

6.2. Simulation results

To assess our protocols, a performance comparison with the following three reference protocols is considered:

- Activity-Rate-Aware (ARA) protocol: this protocol was proposed in Bany Salameh et al. (2020) which considers the bottleneck rate in routing, in addition to PUs activity. Unfortunately, this protocol does not consider jammers activity and also does not consider the required number of time shares when FD technology is used.
- Activity-Sharing-Aware (ASA) protocol: this protocol was proposed in Bany Salameh (2020) which considers the required number of time shares when routing in addition to PUs activity. However, this protocol does not consider jammers activity and the bottleneck-data rate.
- Activity-Sharing-Rate-Aware (ASRA) protocol: this protocol is the combination of the aforementioned two protocols that considers both bottleneck-data rate and the required number of time shares for route discovery, in addition to PUs activity.

Note that, in the conducted experiments, for all proposed and existing protocols, the effective end-to-end throughput for a given

Table 3
Main Simulation Parameters.

Parameter	Value
Area	500 m × 500 m
Number of SUs	100
Number of channels	10
SU's transmission range	100 m
Data packet length	2 KB
Data rate	(40–80) Mbps
Channels average idle duration	5, 100, 30, 5, 45, 50, 100, 5, 45, 30 ms
Channels average jamming duration	5, 0.7, 5, 2, 10, 5, 1, 2.9, 20, 0.3 ms

path is calculated as the rate for the link with the minimum data rate (calculated as the packet size divided by transmission time) divided by the required number of sharing times over this investigated path.

6.2.1. The impact of jamming severity

In our simulation experiments, we first studied the impact of jamming severity, because we need to determine the values of the jamming severity indicator, Ψ, that corresponds to high, medium, and low jamming activities. These values are used in the next subsections when other network parameters are studied, such as PUs' activity and number of licensed channels. Figs. 7 and 8 show the effective throughput with respect to jamming severity factor, Ψ, when number of channels is 6 and 10, respectively. Obviously, when the probability of a channel being idle is low, $P_{idle} = 0.1$, all protocols have the same performance with a very low throughput. However, if P_{idle} is 0.5 and 0.9, our proposed jamming-aware protocols outperform jamming-unaware protocols. On the other hand, the highest improvement occurs when jamming is severe, e.g.; $\Psi = 0.01$, and the improvement becomes fixed when Ψ becomes greater than 1. Also, results show that the improvement is moderate when Ψ is 0.3. Thus, for next subsection, we consider high, moderate, and low jamming severity occurs when Ψ is 0.01, 0.3, and 1, respectively.

6.2.2. The impact of primary users activity

The probability of a channel being idle depends on its PU's activity, e.g.; when PU's activity is low, then, P_{idle} is high. In this work, the effect of P_{idle} on the effective throughput is studied with low, moderate, and high jamming severities. Figs. 9 and 10 show the throughput for low, moderate, and high jamming severities when number of channels is 6 and 10, respectively. Results show that when jamming is high our proposed jamming-aware protocols outperform the other jamming-unaware protocols. This is expected because our protocols are jamming aware, and their improvement shows up when jamming severity increases. In Fig. 9. (c), the throughput improvement is up to 112%, e.g.; when P_{idle} is 0.5 and 0.7, the throughput is improved by 90% and 100%, respectively.

6.2.3. The impact of number of licensed channels

The number of licensed channels in the network affects the average effective throughput, in this subsection, extensive experiments were conducted while the jamming severity and the probability of a channel being idle were both varied. Fig. 11 shows the effective throughput versus number of channels when jamming severity is high, $\Psi = 0.01$. In Fig. 11. (a), when channels availability is low (high PUs activity), $P_{idle} = 0.1$, all protocols has the same very low performance. However, when channels availability becomes moderate, P_{idle} is 0.5, Fig. 11. (b), our proposed jamming-aware protocols outperform the existing three jamming-unaware protocols by up to 134%. Further, when channels' availability is high, P_{idle} is 0.9, Fig. 11. (c), our proposed jamming-aware protocols significantly outperform the existing three jamming-unaware protocols by up to 127%. Figs. 12 and 13

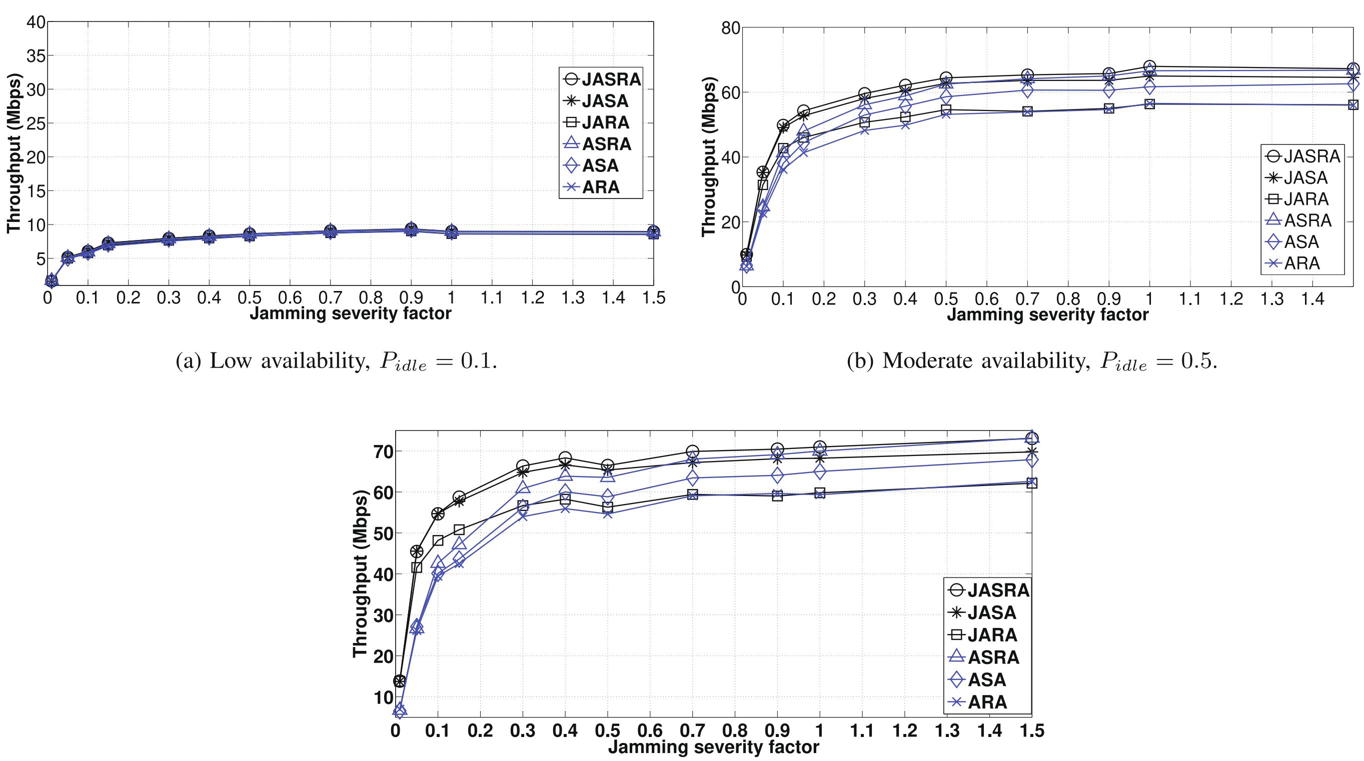

(a) Low availability, $P_{idle} = 0.1$.

(b) Moderate availability, $P_{idle} = 0.5$.

(c) High availability, $P_{idle} = 0.9$.

Fig. 7. The effective throughput versus jamming severity factor, Ψ, when number of channels = 6.

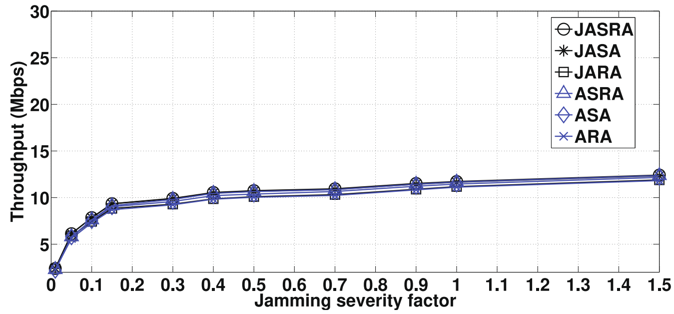

(a) Low availability, $P_{idle} = 0.1$.

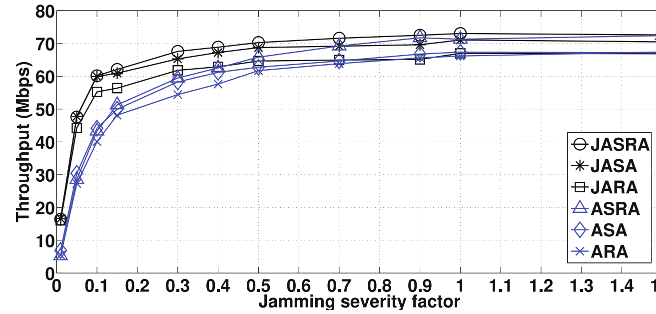

(b) Moderate availability, $P_{idle} = 0.5$.

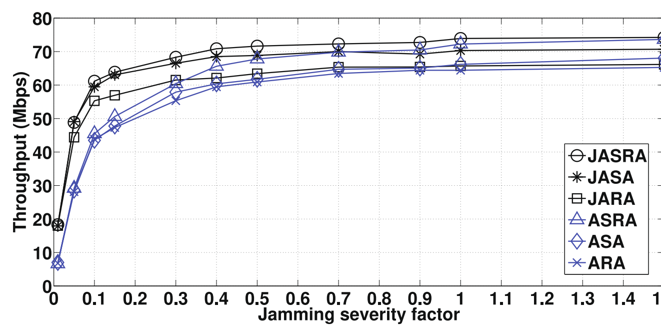

(c) High availability, $P_{idle} = 0.9$.

Fig. 8. The effective throughput versus jamming severity factor, Ψ, when number of channels = 10.

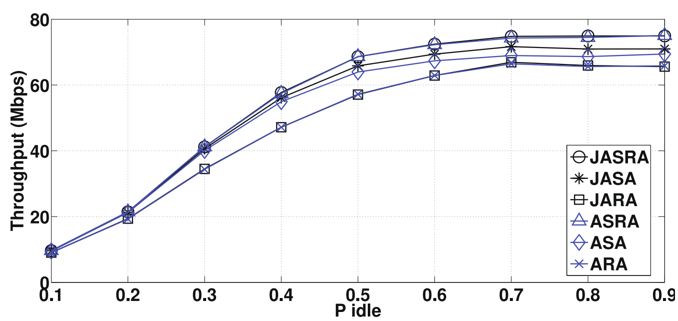

(a) Low Jamming, $\Psi = 1$.

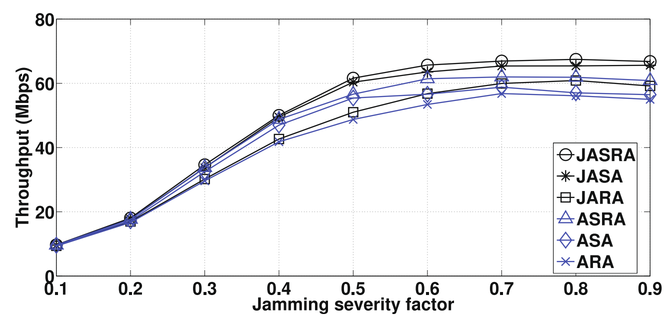

(b) Moderate Jamming, $\Psi = 0.3$.

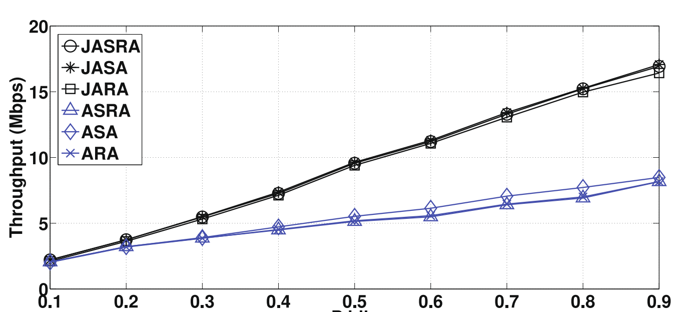

(c) High Jamming, $\Psi = 0.01$.

Fig. 9. The effective throughput versus probability of channels availability, P_{idle}, when number of channels = 6.

show the same trends as discussed for Fig. 11. However, the effective throughput is highest when jamming severity is low, and is lowest when jamming severity is high. This is because when jamming inter-arrival time is low (high jamming), the SUs transmission gets corrupted, i.e.; established paths' failure occurs due to jamming packets' interference. Plus, notice that the effective

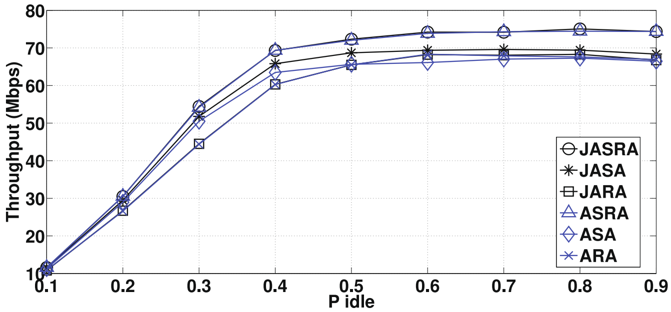

(a) Low Jamming, $\Psi = 1$.

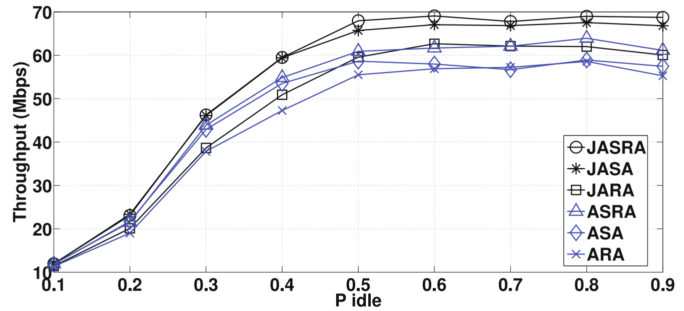

(b) Moderate Jamming, $\Psi = 0.3$.

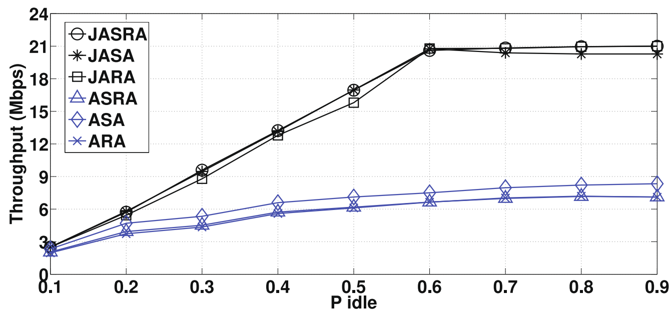

(c) High Jamming, $\Psi = 0.01$.

Fig. 10. The effective throughput versus probability of channels availability, P_{idle}, when number of channels = 10.

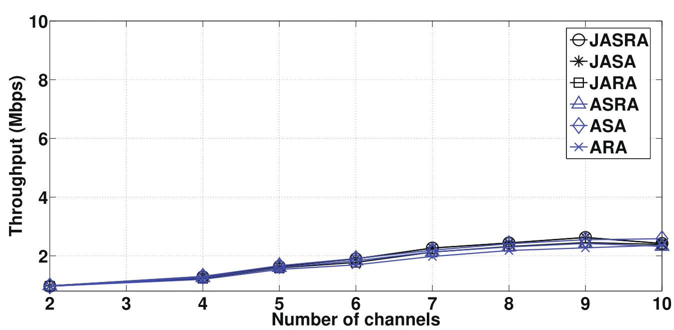

(a) Idle probability, $P_{idle} = 0.1$.

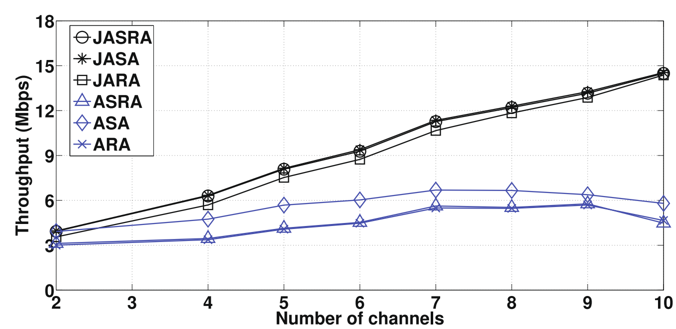

(b) Idle probability, $P_{idle} = 0.5$.

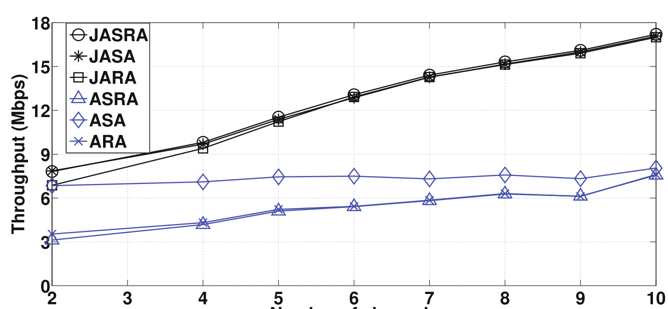

(c) Idle probability, $P_{idle} = 0.9$.

Fig. 11. The effective throughput versus number of channels for different idle probabilities under high jamming, $\Psi = 0.01$.

throughput increases when jamming severity decreases, therefore, the throughput in Fig. 13 is greater than that in Fig. 12. In summary, noting that when the probability of channels availability is low, $P_{idle} = 0.1$, (i.e., the average number of available channels is low), the achieved throughput is low regardless of the smartness of our proposed three routing protocols.

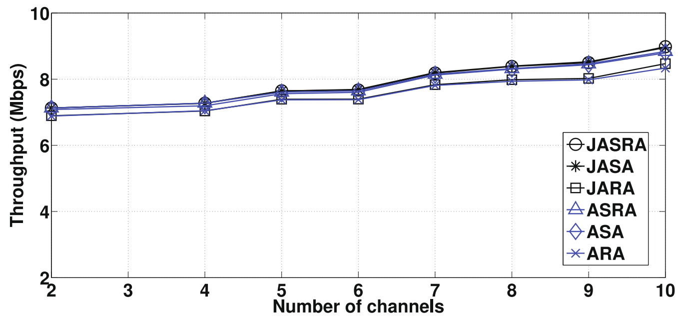

(a) Idle probability, $P_{idle} = 0.1$.

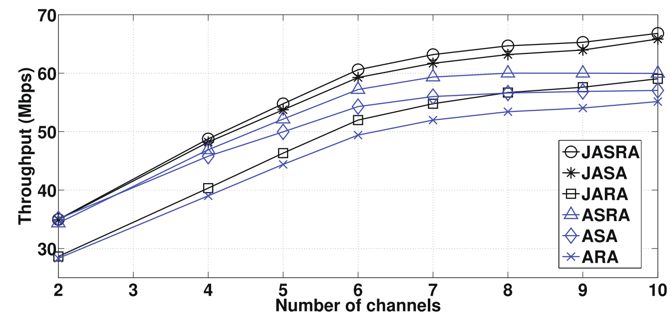

(b) Idle probability, $P_{idle} = 0.5$.

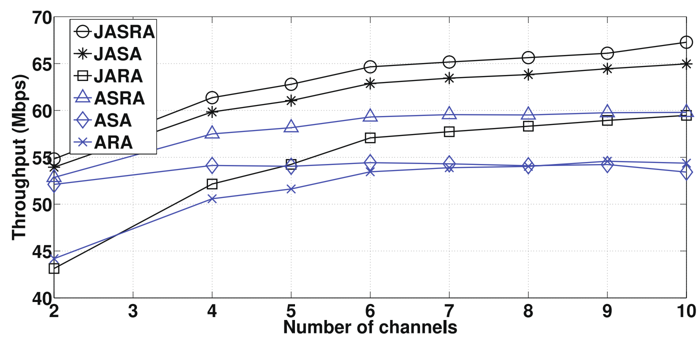

(c) Idle probability, $P_{idle} = 0.9$.

Fig. 12. The effective throughput vs. number of channels for different idle probabilities under moderate jamming, $\Psi = 0.3$.

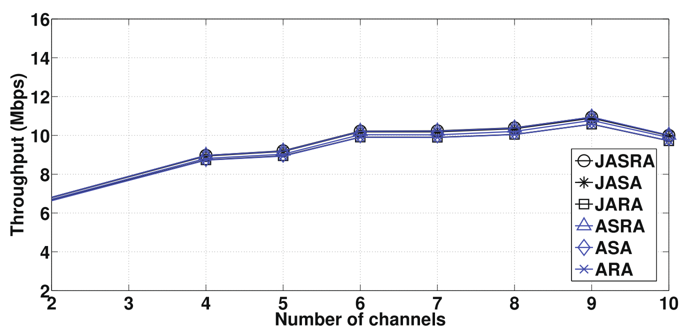

(a) Idle probability, $P_{idle} = 0.1$.

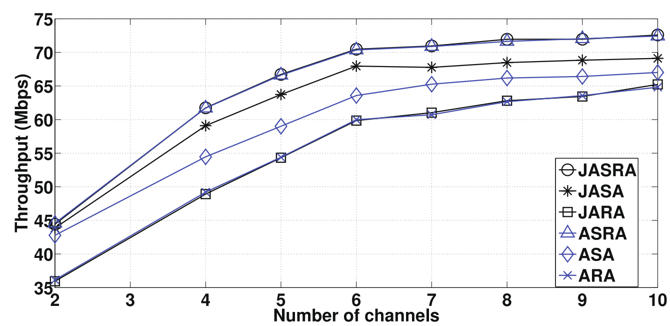

(b) Idle probability, $P_{idle} = 0.5$.

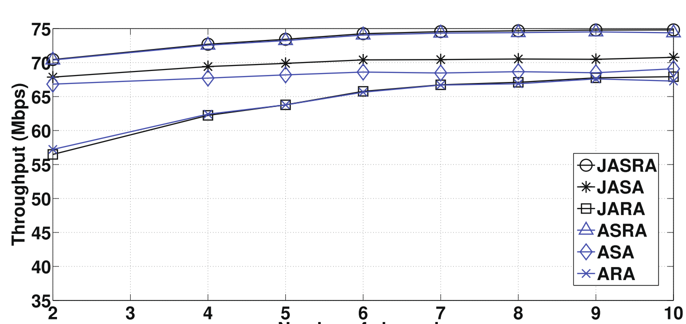

(c) Idle probability, $P_{idle} = 0.9$.

Fig. 13. The effective throughput vs. number of channels for different idle probabilities when jamming is low, $\Psi = 1$.

6.2.4. Number of established paths

To demonstrate the fairness of results that compare between our proposed protocols and the existing protocols, the number of successfully established paths were evaluated for all conducted simulation experiments. However, we present only three sample results, because all results have the same trend. Fig. 14. (a) shows

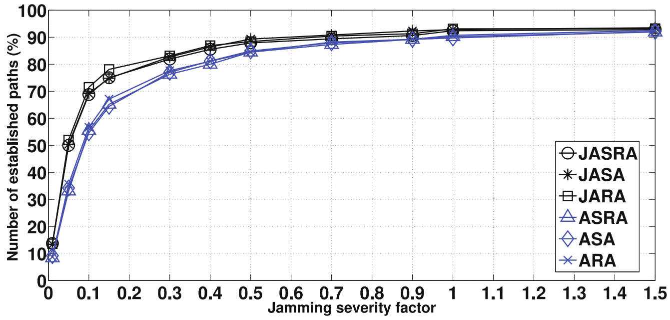

(a) Number of channels is 6 and $P_{idle} = 0.5$.

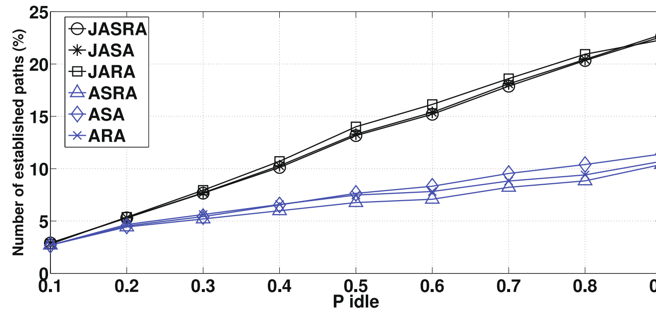

(b) Number of channels is 6 and high jamming severity.

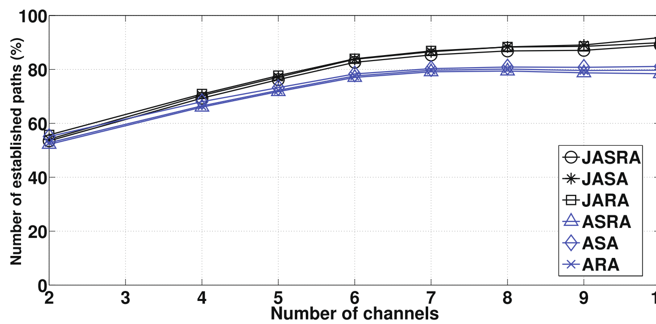

(c) Idle probability, $P_{idle} = 0.5$, and moderate jamming severity.

Fig. 14. Number of established paths vs. jamming severity, Ψ, probability of channels being idle and number of channels.

a sample result of the number of established paths versus jamming severity factor, Ψ, when number of channels is 6 with moderate channels availability, $P_{idle} = 0.5$. Fig. 14. (b) shows a sample result for the number of established paths versus the probability of a channel being idle, P_{idle}, when the number of channels is 6 with high jamming severity, $\Psi = 0.01$. Fig. 14. (c) shows a sample result for the number of established paths versus the number of channels for moderate channels availability, $P_{idle} = 0.5$, and moderate jamming severity, $\Psi = 0.3$.

These figures' results show that the number of established paths, for the three proposed jamming-aware protocols (*JASRA*, *JASA*, and *JARA*), is comparable. Also, the number of established paths is comparable for the three jamming-unaware protocols (*ASRA*, *ASA*, and *ARA*). On the other hand, the number of established paths for our proposed three jamming-aware routing protocols is higher than the other three jamming-unaware routing protocols. This can be justified by the fact that the number of routing failures for jamming aware protocols is less than jamming unaware protocols, because jamming existence is not considered in earlier protocols. On the other hand, although when routing protocols, e.g.; our three proposed protocols, have the same number of established paths, their routing performance, e.g.; effective throughput, is different based on the efficiency of the adopted routing metrics, as previously demonstrated in this section.

7. Conclusions

In Cognitive Radio Networks (CRNs), discovering a route with the highest probability of successful transmission is challenging, because of multiple factors, such as the achieved transmission data rate, PUs' activity, jammers activity, and the number of required time shares which varies for each possible route. This work was strongly motivated to propose three routing protocols in CRNs, where the aforementioned factors are completely studied and combined with FD transmission technology. These protocols are Jamming-Activity-Sharing-Rate-Aware (JASRA) protocol, Jamming-Activity-Rate-Aware (JARA) protocol, and Jamming-Activity-Sharing-Aware (JASA) protocol. The *MLHG* is used in our proposed routing protocols, and it is converted to a simple graph, namely *HLG*, to facilitate the route discovery process. Interestingly, in this model, the complexity to find the best route is a polynomial-time problem (unlike the NP-hard time complexity of the optimization-based existing protocols). Extensive simulation experiments were conducted, in which the proposed routing protocols showed significant throughput improvements over three existing routing protocols, namely, Activity-Rate-Aware (ARA) protocol, Activity-Sharing-Aware (ASA) protocol, and Activity-Sharing-Rate-Aware (ASRA) protocol. As future work, we plan to extend our proposed protocol by incorporating artificial intelligence mechanisms to accommodate for hybrid unknown smart jamming attacks.

Declaration of Competing Interest

The authors declare that they have no known competing financial interests or personal relationships that could have appeared to influence the work reported in this paper.

References

Aghaei, F., Avokh, A., 2020. MRCSC: A cross-layer algorithm for joint Multicast Routing, Channel selection, Scheduling, and Call admission control in multi-cell multi-channel multi-radio cognitive radio WMNS. Pervasive Mobile Comput. 64.

Ahmed, E., Eltawil, A., 2015. All-digital self-interference cancellation technique for full-duplex systems. IEEE Trans. Wireless Commun. 14 (7), 3519–3532.

Almasaeid, H., Al-Kofahi, O., Alnabelsi, S.H., Saifan, R., 2019. Tree-based multicast service provisioning with maximum immunity in cognitive radio networks. J. High Speed Networks 25 (4), 367–384.
Alnabelsi, S.H., 2017. Finding an immuned path against single primary user activity in cognitive radio networks. Int. J. Commun. Antenna Propag 7 (7), 562–571.
Alnabelsi, S.H., Kamal, A.E., 2013. Resilient multicast routing in CRNs using a multilayer hyper-graph approach. In: IEEE international conference on communications (ICC), pp. 2910–2915.
Amjad, M., Akhtar, F., et al., 2017. Full-duplex communication in cognitive radio networks: A survey. IEEE Commun. Surveys Tutor. 19 (4), 2158–2191.
Badarneh, O., Bany Salameh, H., 2011. Opportunistic routing in cognitive radio networks: Exploiting spectrum availability and rich channel diversity. IEEE Global Telecommunications Conference, 1–5.
Bany Salameh, H., 2020. Quantifying the Impact of Time-sharing on Route Capacity in Cognitive Radio Networks with Full-Duplex Capability. IEEE Commun. Lett. 25 (1), 94–98.
Bany Salameh, H., Abusamra, R., 2021. Intelligent multicast routing for multimedia over cognitive radio networks: a probabilistic approach. Multimedia Tools Appl. 80 (11), 1–12.
Bany Salameh, H., AL-Quraan, M., 2020. Securing delay-sensitive CR-IoT networking under jamming attacks: parallel transmission and batching perspective. IEEE Internet Things J.
Bany Salameh, H., El-Khatib, R., 2018. Spectrum-Aware Routing in Full-Duplex Cognitive Radio Networks: An Optimization Framework. IEEE Syst. J., 99, 1–9.
Bany Salameh, H., Otoum, S., et al., 2020. Intelligent jamming-aware routing in multi-hop IoT-based opportunistic cognitive radio networks. Ad Hoc Netw. 98, 102035.
Bany Salameh, H., Kasasbeh, H., Harb, B., 2016. An Opportunistic Guard-band-aware Channel Assignment: A batch-based Approach. In: Proc. of the IEEE WCNC'16 Conference, Qatar. pp. 1–6, April 2016.
Bany Salameh, H., Almajali, S., Ayyash, M., Elgala, H., 2018. Spectrum assignment in cognitive radio networks for internet-of-things delay-sensitive applications under jamming attacks. IEEE Internet Things J. 5 (3), 1904–1913.
Bany Salameh, H., Qawasmeh, R., Al-Ajlouni, A.F., 2020. Routing with intelligent spectrum assignment in full-duplex cognitive networks under varying channel conditions. IEEE Commun. Lett. 24 (4), 872–876.
Bany Salameh, H., Al-Nusair, N., Alnabelsi, S.H., Darabkh, K.A., 2020. Channel assignment mechanism for cognitive radio network with rate adaptation and guard band awareness: batching perspective. Wireless Netw. 26 (6), 4477–4489.
Bayrakdar, M., Çalhan, A., 2017. Non-preemptive queueing model of spectrum handoff scheme based on prioritized data traffic in cognitive wireless networks. ETRI J. 39 (4), 558–569.
Bayrakdar, M., Çalhan, A., 2018. Artificial bee colony-based spectrum handoff algorithm in wireless cognitive radio networks. Int. J. Commun. Syst. 31, (5) e3495.
Bharadia, D., McMilin, E., Katti, S., 2013. Full duplex radios. In: Proceedings of the ACM SIGCOMM conference on SIGCOMM. pp. 375-386.
Boccaletti, S., Ginestra, B., et al., 2014. The structure and dynamics of multilayer networks. Phys. Rep. 544 (1), 1–122.
Cicioğlu, M., Bayrakdar, M., Çalhan, A., 2019. Performance analysis of a new MAC protocol for wireless cognitive radio networks. Wireless Pers. Commun. 108 (1), 67–86.
Darabkh, K.A., Amro, O.M., et al., 2020. JavaSim-IBFD-CRNs: Novel Java simulator for In-Band Full-Duplex Cognitive Radio Networks over Internet of Things Environment. J. Network Comput. Appl. 172, 102833.
Darabkh, K.A., Amro, O., Bany Salameh, H., Al-Zubi, R., 2019. A-Z overview of the in-band full-duplex cognitive radio networks. Comput. Commun. 145, 66–95.
Darabkh, K.A., Amro, O., Al-Zubi, R.T., Bany Salameh, H., 2020. Yet efficient routing protocols for half-and full-duplex cognitive radio Ad-Hoc Networks over IoT environment. J. Network Comput. Appl. 173, 102836.
Furqan, H., Aygül, M.A., Nazzal, M., Arslan, H., 2020. Primary user emulation and jamming attack detection in cognitive radio via sparse coding. EURASIP J. Wireless Commun. Networking 1, 1–19.
Gecgel, S., Goztepe, C., Kurt, G., 2019. Jammer detection based on artificial neural networks: A measurement study. In: Proceedings of the ACM Workshop on Wireless Security and Machine Learning. pp. 43-48.
Hanawal, M., Nguyen, D., Krunz, M., 2019. Cognitive networks with in-band full-duplex radios: Jamming attacks and countermeasures. IEEE Trans. Cogn. Commun. Networking 6 (1), 296–309.
Hassan, M., Karmakar, G.C., Kamruzzaman, J., Srinivasan, B., 2017. Exclusive use spectrum access trading models in cognitive radio networks: A survey. IEEE Commun. Surveys Tutor. 19 (4), 2192–2231.
Hua, M., Yang, L., Pan, C., Nallanathan, A., 2019. Throughput maximization for full-duplex UAV aided small cell wireless systems. IEEE Wireless Commun. Lett. 9 (4), 475–479.
IEEE Std 802.22-2011, pp. 1680, Active, July 2011.
Kadhim, A., Seno, S., 2019. Energy-efficient multicast routing protocol based on SDN and fog computing for vehicular networks. Ad Hoc Netw. 84, 68–81.
Math Works. [Online]. http://www.mathworks.com.
McGee, F., Ghoniem, M., et al., 2019. The state of the art in multilayer network visualization. Computer Graphics Forum 38 (6), 125–149.
Miazi, M., Tabassum, M., et al., 2015. An energy-efficient common control channel selection mechanism for cognitive radio ad-hoc networks. Ann. Telecommun. 70 (1), 11–28.
Mikko, K., Arenas, A., et al., 2014. Multilayer networks. J. Complex Networks 2 (3), 203–271.
Nguyen, B., Tran, X.N., 2020. Transmit antenna selection for full-duplex spatial modulation multiple-input multiple-output system. IEEE Syst. J. 14 (4), 4777–4785.
Qureshi, S., Ahmad, S., Ikram, A., Hasan, N., 2016. Joint energy and throughput based multi-channel assignment in cognitive radio sensor network. In: 2016 IEEE 3rd International Symposium on Telecommunication Technologies (ISTT), pp. 65–69.
Rajkarnikar, N., Peha, J.M., Aguiar, A., 2017. Location privacy from dummy devices in database-coordinated spectrum sharing. In: IEEE International Symposium on Dynamic Spectrum Access Networks (DySPAN). pp. 1–10.
Sarret, M., Berardinelli, G., et al., 2016. Analyzing the potential of full duplex in 5G ultra-dense small cell networks. EURASIP J. Wireless Commun. Netw. 1, 1–16.
Shi, Y., Sagduyu, Y.E., et al., 2018. Adversarial deep learning for cognitive radio security: Jamming attack and defense strategies. In: 2018 IEEE International Conference on Communications Workshops (ICC Workshops), pp. 1–6.
Shu, T., Cui, S., Krunz, M., 2006. Medium access control for multi-channel parallel transmission in cognitive radio networks. IEEE Globecom, 1–5.
Thilina, K. et al., 2015. DCCC-MAC: A dynamic common-control-channel-based MAC protocol for cellular cognitive radio networks. IEEE Trans. Veh. Technol. 65 (5), 3597–3613.
Wei, Z.-H., Hu, B.-J., 2018. A fair multi-channel assignment algorithm with practical implementation in distributed cognitive radio networks. IEEE Access 6, 14255–14267.
Yousaf, A., Loan, A., et al., 2017. Physical-layer intrusion detection system for smart jamming attacks. Trans. Emerg. Telecommun. Technol. 28 (11), e3189.